

## Spin-locked multiple quantum coherence for signal enhancement in heteronuclear multidimensional NMR experiments

Stephan Grzesiek and Ad Bax

*Laboratory of Chemical Physics, National Institute of Diabetes and Digestive and Kidney Diseases,  
National Institutes of Health, Bethesda, MD 20892-0520, U.S.A.*

Received 14 June 1995

Accepted 13 August 1995

**Keywords:** Multidimensional NMR; Line narrowing; Relaxation; Multiple quantum coherence; ROESY; Protein; Calmodulin

### Summary

For methine sites the relaxation rate of  $^{13}\text{C}$ - $^1\text{H}$  two-spin coherence is generally slower than the relaxation rate of the individual  $^{13}\text{C}$  and  $^1\text{H}$  single spin coherences. The slower decay of two-spin coherence can be used to increase the sensitivity and resolution in heteronuclear experiments, particularly those that require correlation of  $\text{H}^\alpha$  and  $\text{C}^\alpha$  chemical shifts. To avoid dephasing of the two-spin coherence caused by  $^1\text{H}$ - $^1\text{H}$  J-couplings, the  $^1\text{H}$  spin is locked by the application of a weak rf field, resulting in a spin-locked multiple quantum coherence. For a sample of calcium-free calmodulin, use of the multiple quantum approach yields significant signal enhancement over the conventional constant-time 2D HSQC experiment. The approach is applicable to many multidimensional NMR experiments, as demonstrated for a 3D  $^{13}\text{C}$ -separated ROESY CT-HMQC spectrum.

The large one-bond  $^1\text{H}$ - $^{13}\text{C}$  dipolar interaction is usually the main source of relaxation for  $^{13}\text{C}$  nuclei in diamagnetic proteins. This dipolar interaction has a magnitude comparable to that between two geminal methylene protons and also dominates relaxation of  $^{13}\text{C}$ -attached methine protons. It is well known that in the slow tumbling limit, the decay of  $^1\text{H}$ - $^{15}\text{N}$  or  $^1\text{H}$ - $^{13}\text{C}$  two-spin coherence is, to first order, not affected by this dipolar coupling (Griffey and Redfield, 1987). Although this feature has found useful application in  $^{15}\text{N}$ - $^1\text{H}$  NMR (Bax et al., 1989; Billeter et al., 1992; Kuboniwa et al., 1994),  $^{13}\text{C}$  line widths obtained from a heteronuclear multiple quantum correlation (HMQC) experiment for  $^1\text{H}^\alpha$ - $^{13}\text{C}^\alpha$  of proline residues in the protein staphylococcal nuclease did not show any improvement over those observed in the corresponding heteronuclear single quantum correlation (HSQC) experiment (Bax et al., 1990). As was pointed out in that study, the presence of homonuclear  $^1\text{H}$ - $^1\text{H}$  J-modulation in the HMQC experiment results in unresolved multiplet patterns in the  $^{13}\text{C}$  dimension, offsetting the gain in resolution caused by the slower relaxation rate. Grzesiek et al. (1995) recently exploited the  $^1\text{H}$ - $^1\text{H}$  J-modulation of the slowly relaxing multiple quantum coherence for measuring  $\text{H}^\alpha$ - $\text{H}^\beta$  J-couplings in  $^{13}\text{C}$ -labeled proteins. Here, we introduce a spin-locked heteronuclear

multiple quantum experiment which is not subject to  $^1\text{H}$ - $^1\text{H}$  J-dephasing, and explore the potential of this concept for sensitivity enhancement.

In the slow tumbling limit, transverse relaxation is dominated by  $J(0)$  terms of the spectral density and, neglecting cross correlation, chemical shift anisotropy, and  $^{13}\text{C}$ - $^{13}\text{C}$ ,  $^{13}\text{C}$ - $^{15}\text{N}$ ,  $^1\text{H}$ - $^{15}\text{N}$ ,  $^1\text{H}$ - $^2\text{H}$  and  $^{13}\text{C}$ - $^2\text{H}$  dipolar interactions, the transverse relaxation rates of  $\text{H}^\alpha$ ,  $\text{C}^\alpha$  and  $\text{H}^\alpha$ - $\text{C}^\alpha$  two-spin coherence are then, to a good approximation, given by:

$$R_H = (1/20) J(0) [4 D_{\text{HC}}^2 + 4 \sum_S D_{\text{HS}}^2 + 5 \sum_I D_{\text{HI}}^2] \quad (1a)$$

$$R_C = (1/20) J(0) [4 D_{\text{HC}}^2 + 4 \sum_I D_{\text{IC}}^2 + \sum_I D_{\text{HI}}^2] \quad (1b)$$

$$R_{\text{MQ}} = (1/20) J(0) [\sum_I (5 D_{\text{HI}}^2 + 4 D_{\text{IC}}^2) + 4 \sum_S D_{\text{HS}}^2] \quad (1c)$$

where the summations extend over all intramolecular protons, I, and carbons, S, other than the proton, H, and carbon, C, under consideration.  $J(0)$  equals the rotational correlation time,  $\tau_c$ , and the dipolar coupling between nuclei x and y is given by  $D_{xy} = h\gamma_x\gamma_y / (2\pi r_{xy}^3)$ , where h is Planck's constant,  $\gamma_x$  is the gyromagnetic ratio of spin x, and  $r_{xy}$  is the x-y internuclear distance. Note that the factor of five instead of nine needs to be used for the proton-proton relaxation term in Eq. 1a, since the pro-

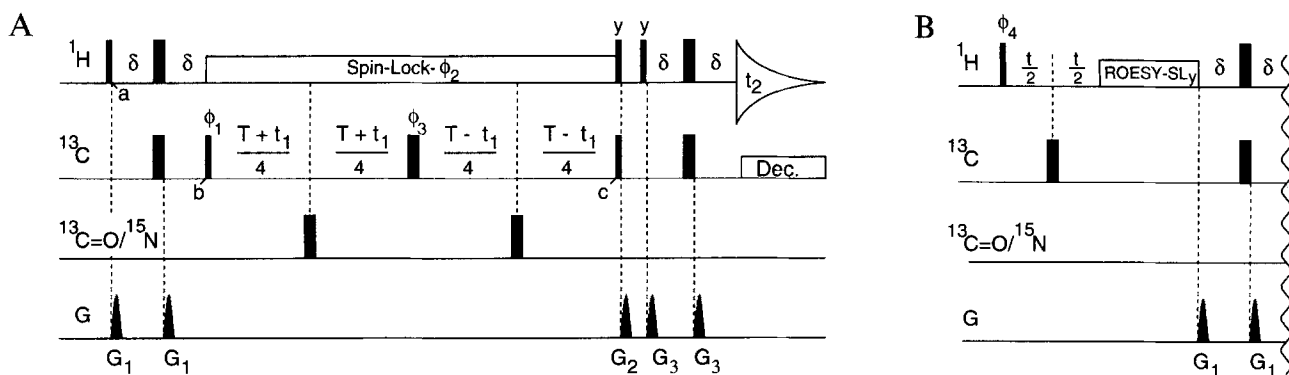


Fig. 1. (A) Pulse scheme for the 2D constant-time HMQC experiment; and (B) the additional pulses needed to transform the 2D CT-HMQC experiment into a 3D  $^{13}\text{C}$ -separated ROESY CT-HMQC experiment. Narrow and wide bars correspond to flip angles of  $90^\circ$  and  $180^\circ$ , respectively. Unless indicated, all pulses are applied along the x-axis. High-power  $^1\text{H}$  pulses are applied using  $\gamma B_1 = 25$  kHz;  $^{13}\text{C}$  pulses (carrier at 46 ppm) are applied using  $\gamma B_2 = 22$  kHz;  $^{13}\text{CO}$   $180^\circ$  pulses (carrier at 177 ppm) are sine-bell shaped and have a duration of  $300 \mu\text{s}$ ;  $^{15}\text{N}$  pulses (carrier at 116.5 ppm) are applied using  $\gamma B_3 = 5.5$  kHz. The  $^1\text{H}$  spin-lock field ( $\gamma B_4 = 6.25$  kHz) is of phase  $\phi_2 = x$ . Because of the difference in power level between the high power and the  $^1\text{H}$  spin-lock fields, it is important to adjust  $\phi_2$  such that it corresponds to phase  $x$  in the high-power mode. Delay durations:  $\delta = 1.5$  ms,  $T = 6.9$  ms or  $13.6$  ms. Gradients are sine-bell shaped with a strength of  $25$  G/cm at their center and have durations:  $G_{1,2,3} = 0.125, 1.5, 0.3$  ms. For the 3D CT-HMQC ROESY experiment, the pulses shown in (B) replace the pulses preceding time point  $b$  in (A), and the delay  $t$  is the incrementable delay for the third ( $^1\text{H}$ ) dimension. Phase cycling for scheme (A):  $\phi_1 = x, -x$ ;  $\phi_2 = x, x, -x, -x$ ;  $\phi_3 = 4(x), 4(-x)$ ;  $\text{Acq.} = x, -x$ . Phase cycling for scheme (B):  $\phi_1 = x, -x$ ;  $\phi_2 = x, x, -x, -x$ ;  $\phi_3 = x$ ;  $\phi_4 = 4(x), 4(-x)$ ;  $\text{Acq.} = x, -x, x, -x, -x, x, -x, x$ . Quadrature in the indirectly detected  $^1\text{H}$  ( $t$ ) and  $^{13}\text{C}$  ( $t_1$ ) dimensions is obtained by States-TPPI phase cycling of  $\phi_4$  and  $\phi_1$ , respectively. In order to reduce  $^1\text{H}$  resonance offset effects during the  $^1\text{H}$  spin-lock, which can reintroduce a scaled heteronuclear J-coupling in the  $^{13}\text{C}$  dimension of the spectrum (cf. Eq. 4), two high-power  $^1\text{H}$   $180^\circ$  pulses can be inserted (not shown) in the pulse scheme such that their positions coincide with the  $^{13}\text{CO}$  and  $^{15}\text{N}$   $180^\circ$  pulses. Use of these additional pulses increases magnetization loss caused by homonuclear Hartmann-Hahn effects and was found to be of no advantage in the application to calmodulin.

tions have different chemical shifts and therefore are 'unlike' (Goldman, 1988). The rate,  $R_C$ , in Eq. 1b applies to the case of freely precessing  $^{13}\text{C}$  magnetization which evolves from anti- to in-phase magnetization, and vice versa. Thus,  $R_C$  is the average between the rates applicable for in-phase and anti-phase  $^{13}\text{C}$  transverse magnetization, again only including  $J(0)$  terms.

In order to evaluate the relative importance of the various dipolar terms in Eq. 1, we have calculated these explicitly for all non-glycine  $\text{C}^\alpha$  and  $\text{H}^\alpha$  spins in bovine pancreatic trypsin inhibitor (BPTI), using X-ray coordinates at  $1.1 \text{ \AA}$  resolution (Parkin et al., 1995). This yields:

$$\langle \sum_i r_{\text{HI}}^{-6} \rangle^{-1/6} = 1.97 \pm 0.13 \text{ \AA} \quad (1.86 \pm 0.10 \text{ \AA}) \quad (2a)$$

$$\langle \sum_{\text{S} \neq \text{C}} r_{\text{HS}}^{-6} \rangle^{-1/6} = 1.79 \pm 0.03 \text{ \AA} \quad (2b)$$

$$\langle \sum_{i \neq \text{H}} r_{\text{IC}}^{-6} \rangle^{-1/6} = 1.81 \pm 0.07 \text{ \AA} \quad (1.69 \pm 0.04 \text{ \AA}) \quad (2c)$$

where the numbers in brackets include amide protons in the summation. This yields the following contributions to the relaxation:

$$\langle (5/20) \sum_i D_{\text{HI}}^2 \rangle = 2.47 \times 10^9 \text{ s}^{-2} \quad (3.50 \times 10^9 \text{ s}^{-2}) \quad (3a)$$

$$\langle (4/20) \sum_{\text{S} \neq \text{C}} D_{\text{HS}}^2 \rangle = 0.22 \times 10^9 \text{ s}^{-2} \quad (3b)$$

$$\langle (4/20) \sum_{i \neq \text{H}} D_{\text{IC}}^2 \rangle = 0.20 \times 10^9 \text{ s}^{-2} \quad (0.30 \times 10^9 \text{ s}^{-2}) \quad (3c)$$

In addition, assuming a  $^1\text{H}$ - $^{13}\text{C}$  distance of  $1.09 \text{ \AA}$ , one finds

$$(4/20) D_{\text{HC}}^2 = 4.30 \times 10^9 \text{ s}^{-2} \quad (3d)$$

Substitution of these values into Eq. 1 indicates that, on average,  $R_{\text{MQ}}$  is  $1.7 \pm 0.6$  ( $1.3 \pm 0.4$ ) times slower than  $R_C$  for a sample without (with) amide protons. Note that the proton relaxation rate,  $R_{\text{H}}$ , is slowed down considerably more [ $R_{\text{H}} / R_{\text{MQ}} = 2.4 \pm 0.9$  ( $2.0 \pm 0.7$ ) (Grzesiek et al., 1995)]. Although the gain for the carbon relaxation rate is much smaller than previously suggested by Seip et al. (1992), we demonstrate below that a significant gain is indeed achievable and can result in considerable spectral enhancement.

Figure 1A shows the multiple quantum analog of the regular constant-time HSQC experiment (Santoro and King, 1992; Van de Ven and Philippens, 1992; Vuister and Bax, 1992), where spin-locking of the protons during the carbon constant-time period is used to remove the effect of the  $^1\text{H}$ - $^1\text{H}$  J-dephasing (Allerhand, 1966). This spin-locked constant-time HMQC experiment is of primary use for the study of methine sites. For proteins it can be used to maximize sensitivity for the  $^{13}\text{C}^\alpha$ - $^1\text{H}^\alpha$  region of the heteronuclear shift correlation spectrum. Due to the finite strength of the  $^1\text{H}$  spin-lock field,  $\omega_{\text{SL}}$ , proton off-resonance effects can become important as they reintroduce the effect of the one-bond  $^1\text{H}$ - $^{13}\text{C}$  J-coupling for the  $^1\text{H}$ - $^{13}\text{C}$  multi-quantum coherence. Just prior to turning on the  $^1\text{H}$  spin-lock field, the coherence for a two-spin system is described by  $2\text{H}_x^\alpha \text{C}_y^\alpha$ . For a proton at an offset  $\delta$  from the rf carrier of the  $^1\text{H}$  spin-lock field, a proton coordinate system is chosen such that the new  $z'$ -axis points in the direction of the effective spin-lock field ( $\omega_e = (\delta^2 + \omega_{\text{SL}}^2)^{1/2}$ ), which makes an angle  $\theta$  ( $\theta = \tan^{-1} \omega_{\text{SL}}/\delta$ ) with the static magnetic field. A fraction  $2\text{H}_z^\alpha \text{C}_y^\alpha \sin \theta$  of

$2\mathbf{H}_z^\alpha\mathbf{C}_y^\alpha$  is aligned along the  $z'$ -axis, whereas the component  $2\mathbf{H}_x^\alpha\mathbf{C}_y^\alpha \cos \theta$ , which is orthogonal to the effective spin-lock field, may be ignored as it will rapidly dephase due to rf inhomogeneity. When  $\theta$  approaches  $90^\circ$ ,  $2\mathbf{H}_z^\alpha\mathbf{C}_y^\alpha$  becomes a pure zero and double quantum coherence, with no active J-coupling between  $^1\text{H}^\alpha$  and  $^{13}\text{C}^\alpha$ . In this case  $2\mathbf{H}_z^\alpha\mathbf{C}_y^\alpha$  relaxes at a rate described by Eq. 1c. For  $\theta \neq 90^\circ$ , part of  $2\mathbf{H}_z^\alpha\mathbf{C}_y^\alpha$  is single quantum coherence, and a residual J-coupling between  $^1\text{H}^\alpha$  and  $^{13}\text{C}^\alpha$ , equal to  $J_{\text{CH}} \cos \theta$  (in the limit where  $\omega_{\text{SL}} \gg J_{\text{CH}}$ ) remains. This introduces rephasing of the  $2\mathbf{H}_z^\alpha\mathbf{C}_y^\alpha$  spin operator product during the  $t_1$  evolution period:

$$2\mathbf{H}_z^\alpha\mathbf{C}_y^\alpha \rightarrow 2\mathbf{H}_z^\alpha\mathbf{C}_y^\alpha \cos(\pi J_{\text{CH}} t_1 \cos \theta) - \mathbf{C}_x^\alpha \sin(\pi J_{\text{CH}} t_1 \cos \theta) \quad (4)$$

In principle, the effect of this residual J-coupling can be eliminated by using phase modulation of the  $^1\text{H}$  rf field along the  $\pm x$ -axis, for example in a WALTZ-16 (Shaka et al., 1983) or DIPSI (Shaka et al., 1988) manner. In practice, however, homonuclear Hartmann-Hahn transfer between  $\text{H}^\alpha$  and  $\text{H}^\beta$  spins would in this case lead to a loss in the amplitude of the  $2\mathbf{H}_z^\alpha\mathbf{C}_y^\alpha$  spin operator product. Instead, we prefer to use a relatively strong (5–7 kHz) cw

spin-lock field, with the carrier near the center of the  $\text{H}^\alpha$  spectral region, in such a way that  $\theta$  is close to  $90^\circ$ . This represents a compromise between minimizing the rephasing process of Eq. 4, and simultaneously minimizing the extent to which  $\mathbf{H}_z^\alpha$  components of the spin operator product are transferred into  $\mathbf{H}_z^\beta$ .

The constant-time spin-locked HMQC experiment can be used to enhance the sensitivity of numerous  $^{13}\text{C}$ -separated 3D and 4D experiments. Here, the application to a  $^{13}\text{C}$ -separated ROESY will be demonstrated. This ROESY experiment can provide important information on the  $\text{H}^\alpha$ - $\text{H}^\beta$  distances, thereby aiding in the stereospecific assignment of these resonances (Clare et al., 1991). The pulse scheme is sketched in Fig. 1B. Even very small amounts of homonuclear Hartmann-Hahn transfer can seriously affect the intensity of weak ROE cross peaks, and care needs to be taken to minimize this transfer (Bax and Davis, 1985). Therefore, during the ROE mixing period, the spin-lock irradiation is shifted downfield, to  $\sim 5.8$  ppm. To ensure phase coherence between the HMQC sequence and the ROESY spin-lock, this shifting is accomplished by varying the phase of the spin-lock field linearly with time, without actually moving the rf carrier frequency generated by the console (Kay et al., 1989).

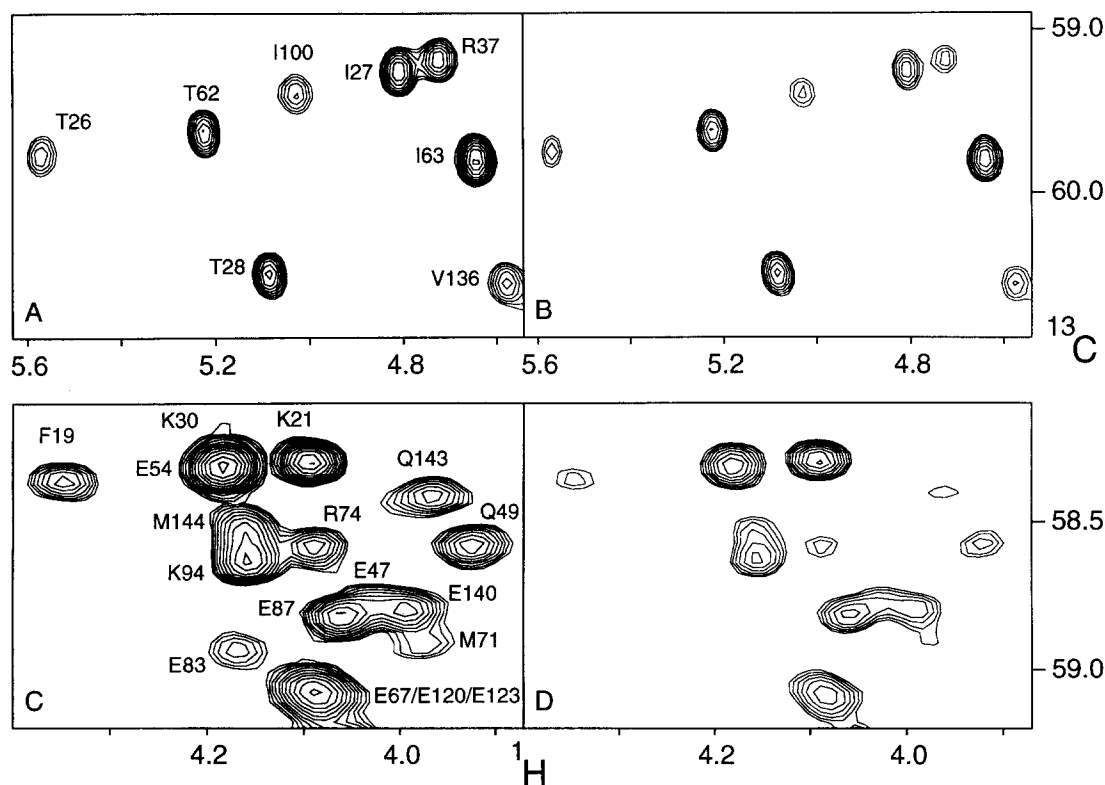


Fig. 2. Comparison of small regions of 600 MHz spin-locked 2D CT-HMQC spectra recorded with (A)  $4T = 28$  ms and (C)  $4T = 56$  ms, with their corresponding regular CT-HSQC spectral regions (B, D) for a sample of 1.5 mM uniformly  $^{13}\text{C}$ -enriched apo-calmodulin in  $\text{D}_2\text{O}$ , pH 6.3,  $23^\circ\text{C}$ . Each of the four spectra results from a  $273^* \times 384^*$  data matrix, acquired with 8 (A, B) or 16 (C, D) scans per complex  $t_1$  increment, using a  $^{13}\text{C}$  spectral width of 69 (A, B) or 34.5 (C, D) ppm and total measuring times of 40 (A, B) and 80 (C, D) min. All four spectra were processed identically. The lowest contours for spectra (A) and (B) are drawn at the same absolute level, which is 1.25 times lower compared to the lowest contour levels in (C) and (D). Note that the noise level is  $2^{1/2}$  times higher in (C) and (D) due to the twofold larger number of scans compared to spectra (A) and (B). Contours are spaced by a factor of 1.25.

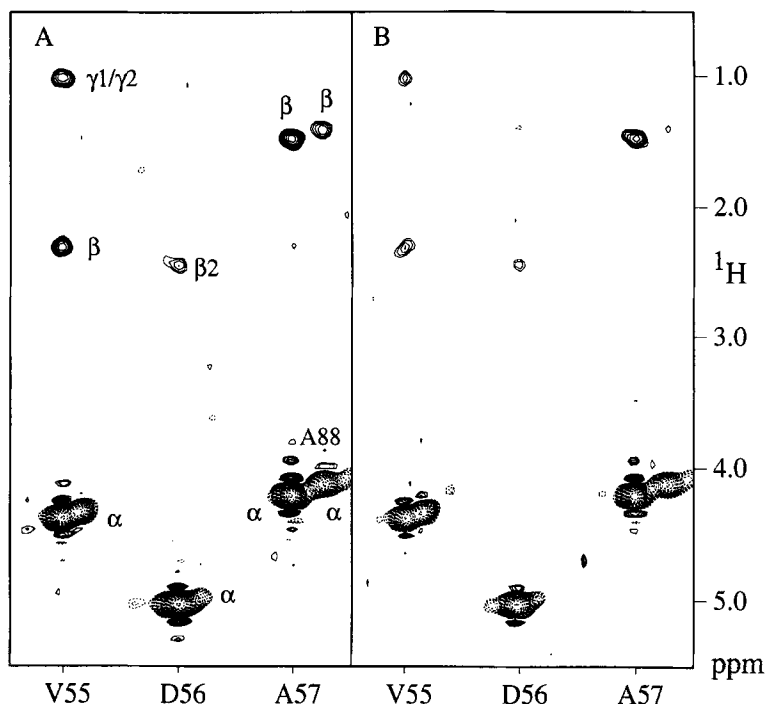


Fig. 3. Comparison of  $^1\text{H}$  strips taken from (A) a 600 MHz spin-locked 3D ROESY CT-HMQC spectrum and (B) the corresponding ROESY CT-HSQC spectrum, taken at the  $^{13}\text{C}^\alpha/{}^1\text{H}^\alpha$  frequencies of residues Val<sup>55</sup>-Ala<sup>57</sup> for a sample of 1.5 mM apo-calmodulin in  $\text{D}_2\text{O}$ , pH 6.3, 23 °C, using a 20-ms ROE mixing period. Each spectrum results from a  $50^* \times 58^* \times 384^*$  data matrix, acquired in 27 h each. Acquisition times in the  $t_1$  ( $^{13}\text{C}$ ),  $t_2$  ( $^1\text{H}$ ) and  $t_3$  ( $^1\text{H}$ ) dimensions are 12, 27 and 53 ms, respectively. Both data sets were processed identically. The lowest contour level is drawn at the same absolute level, and contours are spaced by a factor of 1.25.

Experiments are demonstrated for a sample of calcium-free calmodulin (1.5 mM) in  $\text{D}_2\text{O}$ , pH 6.3, 23 °C. Spectra have been recorded on a Bruker AMX-600 spectrometer, equipped with a triple-resonance 5-mm probehead, containing a self-shielded z-gradient coil. For all experiments, the  $^1\text{H}$  spin-lock field during the  $^{13}\text{C}$  evolution period was between 4 and 6 kHz. The tumbling of calmodulin at 23 °C is anisotropic but, on average, the line widths correspond to that expected for a protein tumbling isotropically with a rotational correlation time of 8 ns (Tjandra et al., 1995).

Figure 2 compares two small regions of the regular CT-HSQC spectrum of calmodulin with the same regions recorded under identical conditions with spin-locked CT-HMQC experiments. For a constant-time duration of 28 ms (Figs. 2A,B), the increase in signal-to-noise is, on average, a factor of 1.4, which corresponds to a decrease in relaxation rate of  $\ln(1.4)/(28 \text{ ms}) = 12 \text{ s}^{-1}$ . This is in good agreement with the difference of  $14 \text{ s}^{-1}$  expected on the basis of Eq. 3, assuming an isotropic correlation time of 8 ns and an order parameter,  $S^2$ , of 0.85. The increase in signal-to-noise ratio for a constant-time duration of 56 ms obtained with the spin-locked CT-HMQC experiment (Fig. 2C) over the regular CT-HSQC experiment (Fig. 2D) averages between two and three. Note that, depending on the position of the proton rf carrier, smaller enhancements are observed for serine and threonine residues, because the similarity of their  $\text{H}^\alpha$  and  $\text{H}^\beta$  chemical

shifts makes it difficult to avoid Hartmann-Hahn matching during the spin-lock pulse.

Figure 3A illustrates the application of the constant-time HMQC experiment to the measurement of a  $^{13}\text{C}$ -separated 3D ROESY spectrum and compares the results with those of a regular ROESY CT-HSQC experiment (Fig. 3B). Both 3D spectra have been recorded with a ROE mixing time of 20 ms, using a 28 ms duration of the constant-time evolution period. The strips compared in Fig. 3 have been taken at the ( $^{13}\text{C}^\alpha, {}^1\text{H}^\alpha$ ) locations of Val<sup>55</sup>-Ala<sup>57</sup> in the 3D spectrum and show cross peaks between the intraresidue  $\text{H}^\alpha$  and  $\text{H}^\beta$  protons. For Val<sup>55</sup>, a cross peak between  $\text{H}^\alpha$  and the overlapping  $\text{H}^\gamma$  protons is also observed. As expected on the basis of the results shown in Fig. 2, the improvement in signal-to-noise ratio is again a factor of  $\sim 1.4$  in the spin-locked HMQC variant of the experiment.

The strong ROE between Val<sup>55</sup>  $\text{H}^\alpha$  and  $\text{H}^\beta$  corresponds to an interproton distance of  $2.2 \pm 0.2 \text{ \AA}$ , suggestive of a gauche arrangement. However, a  $\chi_1 = \pm 60^\circ$  rotamer is not compatible with a large value for  $J(\text{H}^\alpha, \text{H}^\beta)$ , which was measured to be 8.6 Hz before correction for relaxation effects (Grzesiek et al., 1995), and ca. 10 Hz after correction. Interestingly,  $^{15}\text{N}$  relaxation data indicate an exchange process taking place on the microsecond time scale for this residue (Tjandra et al., 1995) and the 4D  $^{13}\text{C}/^{15}\text{N}$ -separated NOESY shows that the amides of both Val<sup>55</sup> and Asp<sup>56</sup> have NOEs of comparable intensities to

both Val<sup>55</sup> methyl groups. This suggests that Val<sup>55</sup> exists as an average of two conformers, with  $\chi_1 \approx 180^\circ$  and  $\chi_1 \approx 0^\circ$ . The  $J(\text{H}^\alpha, \text{H}^\beta)$  value is large for both conformers, but only the  $\chi_1 \approx 0^\circ$  conformer contributes significantly to the ROE buildup. The presence of a C <sup>$\beta$</sup> -branched amino acid (usually phenylalanine) immediately preceding the first calcium-ligating residue (usually aspartate) is a conserved feature in many calcium-binding EF-hand type proteins. Population of the  $\chi_1 = 0^\circ$  conformation in calmodulin is energetically costly and suggests that this residue destabilizes the structure of the calcium-free protein.

Our results presented above provide the first experimental comparison in the slow motion limit of the decay of regular <sup>13</sup>C magnetization with the decay of <sup>13</sup>C magnetization that is part of a heteronuclear two-spin coherence. The average gain in sensitivity obtained experimentally agrees with theoretical predictions, although it is considerably more uniform than expected based on the average <sup>1</sup>H-<sup>1</sup>H dipolar interactions calculated for the H <sup>$\alpha$</sup>  nuclei in BPTI from its 1.1-Å X-ray structure.

The gain in sensitivity of the spin-locked HMQC experiment over that of a regular CT-HSQC increases when the relaxation times are short. Thus, the benefits are largest for slowly tumbling proteins, i.e., where they are needed most. The experiment may also be useful for the study of nucleic acids, where most of the <sup>13</sup>C-attached protons are of the methine type, and the scarcity of protons increases  $\langle \sum_i r_{\text{HI}}^{-6} \rangle^{-1/6}$ , thereby increasing the potential gain of the spin-locked HMQC approach.

Calculations and experimental comparisons indicate that no net gain in relaxation behavior is observed when the spin-locked HMQC experiment in the form described above is applied to methylene and methyl groups. However, other variations of this experiment, which are based on the generation of heteronuclear three- and four-spin coherence, offer the potential for obtaining similar enhancements. Such schemes are presently being evaluated in our laboratory.

## Acknowledgements

This work was supported by the AIDS Targeted Anti-Viral Program of the Office of the Director of the National Institutes of Health.

## References

- Allerhand, A. (1966) *J. Chem. Phys.*, **44**, 1–9.
- Bax, A. and Davis, D.G. (1985) *J. Magn. Reson.*, **63**, 207–213.
- Bax, A., Kay, L.E., Sparks, S.W. and Torchia, D.A. (1989) *J. Am. Chem. Soc.*, **111**, 408–409.
- Bax, A., Ikura, M., Kay, L.E., Torchia, D.A. and Tschudin, R. (1990) *J. Magn. Reson.*, **86**, 304–318.
- Billeter, M., Neri, D., Otting, G., Qian, Y.Q. and Wüthrich, K. (1992) *J. Biomol. NMR*, **2**, 257–274.
- Clore, G.M., Bax, A. and Gronenborn, A.M. (1991) *J. Biomol. NMR*, **1**, 13–22.
- Goldman, M., *Quantum Description of high resolution NMR in Liquids*, Clarendon Press, Oxford, 1988, pp. 248–254.
- Griffey, R.H. and Redfield, A.G. (1987) *Quart. Rev. Biophys.*, **19**, 51–82.
- Grzesiek, S., Kuboniwa, H., Hinck, A. and Bax, A. (1995) *J. Am. Chem. Soc.*, **117**, 5312–5315.
- Kay, L.E., Marion, D. and Bax, A. (1989) *J. Magn. Reson.*, **84**, 72–84.
- Kuboniwa, H., Grzesiek, S., Delaglio, F. and Bax, A. (1994) *J. Biomol. NMR*, **4**, 871–878.
- Parkin, S., Rupp, B. and Hope, H. (1995) entry 1BPI of the Brookhaven Protein Databank, Brookhaven National Laboratory, Upton, NY.
- Santoro, J. and King, G.C. (1992) *J. Magn. Reson.*, **97**, 202–207.
- Seip, S., Balbach, J. and Kessler, H. (1992) *J. Magn. Reson.*, **100**, 406–410.
- Shaka, A.J., Keeler, J., Frenkiel, T. and Freeman, R. (1983) *J. Magn. Reson.*, **52**, 335–338.
- Shaka, A.J., Lee, C.J. and Pines, A. (1988) *J. Magn. Reson.*, **77**, 274–293.
- Tjandra, N., Kuboniwa, H., Ren, H. and Bax, A. (1995) *Eur. J. Biochem.*, **230**, 1014–1024.
- Van de Ven, F.J.M. and Philippens, M.E.P. (1992) *J. Magn. Reson.*, **97**, 637–644.
- Vuister, G.W. and Bax, A. (1992) *J. Magn. Reson.*, **98**, 428–435.